U.S. DEPARTMENT OF COMMERCE
National Oceanic and Atmospheric Administration
Environmental Research Laboratories

NOAA Technical Memorandum ERL NSSL-55

THE NSSL SURFACE NETWORK AND OBSERVATIONS OF HAZARDOUS WIND GUSTS

Operations Staff

National Severe Storms Laboratory
Norman, Oklahoma
June 1971

TABLE OF CONTENTS

THE NSSL SURFACE NETWORK AND OBSERVATIONS OF HAZARDOUS WIND GUSTS

Operations Staff[1]

The NSSL network of surface stations for measurement of meteorological parameters is described. Examples of severe wind conditions recorded with intense thunderstorms are presented in detail, and analyzed wind fields are related to the contoured display of the NSSL WSR-57 radar. The design of an operational system for real time monitoring of wind gust lines is discussed.

1. INTRODUCTION

This report describes the instrumentation and structure of the NSSL surface network and includes analyses of a few of the severe wind gust experiences recorded during the past 2 years. The last section outlines the design of an operational system for real time monitoring of the wind gust lines accompanying severe thunderstorms.

The information contained here supplements Technical Memorandum ERLTM-NSSL 46. The authors are particularly concerned with development of techniques for the identification of severe storm conditions considered hazardous to aviation operations.

The accurate portrayal of the surface winds of thunderstorms generally requires an observing density that is about an order of magnitude greater then is currently available in synoptic data. Special networks (Byers and Braham, 1949; Williams, 1963; Styber and Brown, 1962) have detected pressure patterns ranging from a few miles to a few tens of miles and have provided partial life histories of such systems for periods of about 10 to 100 min. For example, Brown (1962),

---

[1]Contributors to this report are Kenneth E. Wilk, J. T. Dooley, Lester C. Showell, Gerald J. Wardius, John K. Carter, Leonard A. Johnson, and Charles G. Clark.

Fujita (1963), Bonner (1966), and Charba and Sasaki (1968), have extensively analyzed fields of pressure, temperature, wind, and humidity to show continuity in the mesoscale structure of thunderstorm complexes. Although such studies have only partially explained the dynamical processes underlying severe storms, they have shown that many of the events, especially pressure surges and wind gust lines, exhibit conservative properties that are traceable for tens of miles.

In 1969 and 1970, the National Severe Storms Laboratory (NSSL) established a mesoscale network in the vicinity of Oklahoma City to detect and measure the characteristics of gusts accompanying severe thunderstorms. On at least four occasions in April and May 1969 (Barclay and Wilk, 1970; Lemon, 1970), organized squall lines passed over the area causing light to moderate damage to structures and trees. On April 29, 1970, severe damage in northern Oklahoma City resulted from two tornadoes that accompanied large severe thunderstorms. On many other occasions in the past 2 years, local thunderstorms produced heavy rain, hail, and turbulence which affected general aviation operations for 1 to 2 hours. In practically all instances, the storms displayed the radar echo shape or intensity signatures indicative of severe thunderstorms. During these periods, radar data from the NSSL WSR-57 10-cm system and wind velocity data from the surface network were recorded. When analyzed, the data graphically portray the mesoscale air flow patterns in relation to the distribution of storm precipitation.

2. THE NSSL SURFACE NETWORK

In 1969, the network consisted of 29 stations, covered 800 sq miles, and extended from near Chickasha, Oklahoma, northeastward to the vicinity of Edmond, Oklahoma. In 1970, the network was enlarged to 44 stations over 1100 sq miles (fig. 1). The average station spacing during both years was approximately 6 n miles. The center of the 1970 network was in gently rolling terrain, southwest of the Oklahoma City urban area, and had a maximum elevation change of 310 ft over the entire area. Sites were selected to minimize the effect of local terrain, trees, and buildings on wind observations. The irregularities in station spacing result from compromises between exposure and availability of sites in rough or heavily populated areas.

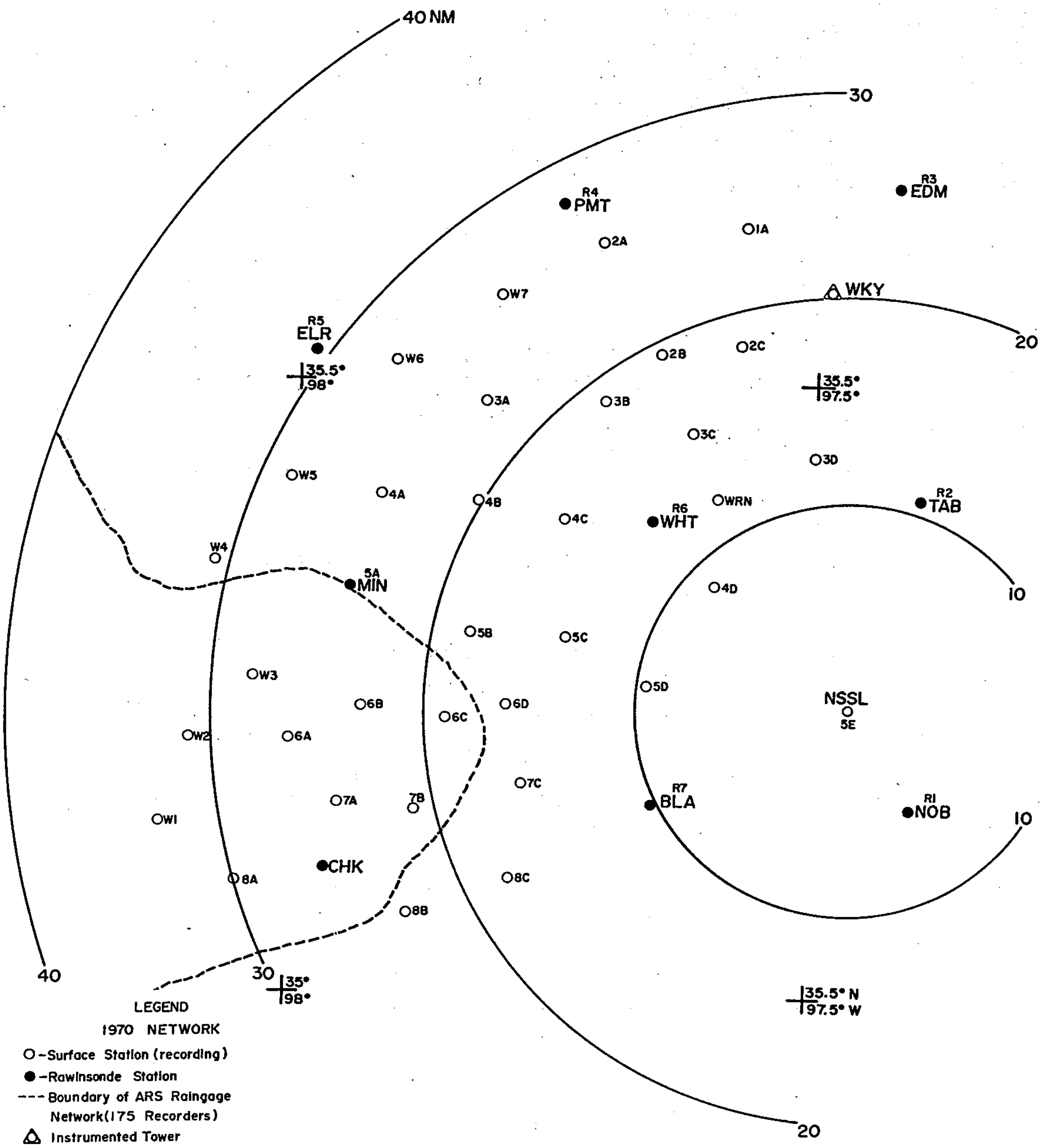

Figure 1. Locations of surface and rawinsonde stations.

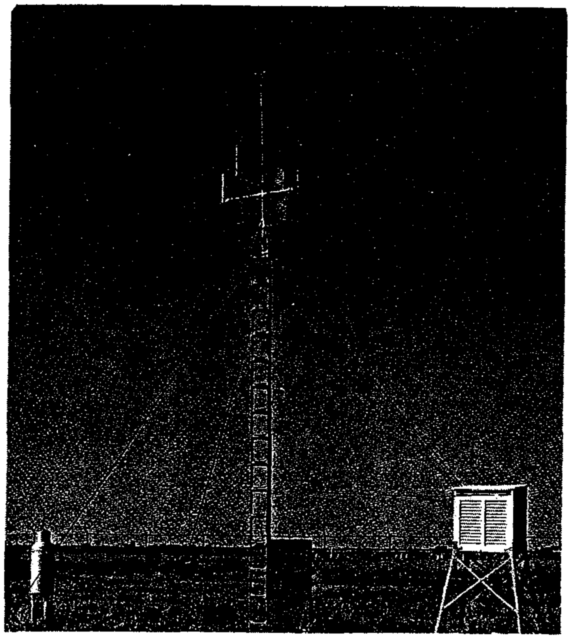

Figure 2. A typical mesonetwork site.

A typical installation is shown in figure 2. The wind vane and cup anemometer are mounted 23 feet above ground level on a triangular tower. There is a recording raingage and the instrument shelter encloses a microbarograph and a hygrothermograph. Table 1 lists the type of equipment and the resolution of the measurements.

Wind direction and speed are recorded on an Esterline Angus analog event recording DC voltmeter. The chart drive on the wind recorder is spring-driven and serves as the master clock for the station. Once each hour, a cam on the wind recorder activates relays which produce simultaneous time marks on the microbarograph, hygrothermograph, and raingage. Examples of network data with time marks are shown in figure 3.

The microbarograph, hygrothermograph, and raingage shown in figure 4 are equipped with spindles so that continuous strip charts can be used. This prevents the trace overwriting, which occurs in the standard instrument with 12-hour gears. Special charts were printed on very thin paper to prevent the significant time errors that would otherwise result from the build-up of the chart on the recorder drum.

Table 1. Equipment at NSSL Network Stations

Parameter	Instrument	Instrument Resolution
Wind direction	F005 (8 point) single vane transmitter	16 points of compass
Wind speed	F420C speed transmitter	± 1.5 kt
Pressure	Belfort Model 5-800 recording microbarograph	± 0.020 inch of mercury
Temperature	Friez Model 594 Hygrothermograph	± 2°F ± 5 percent
Precipitation	Belfort recording raingage Model 5-7775	± 0.04 inch

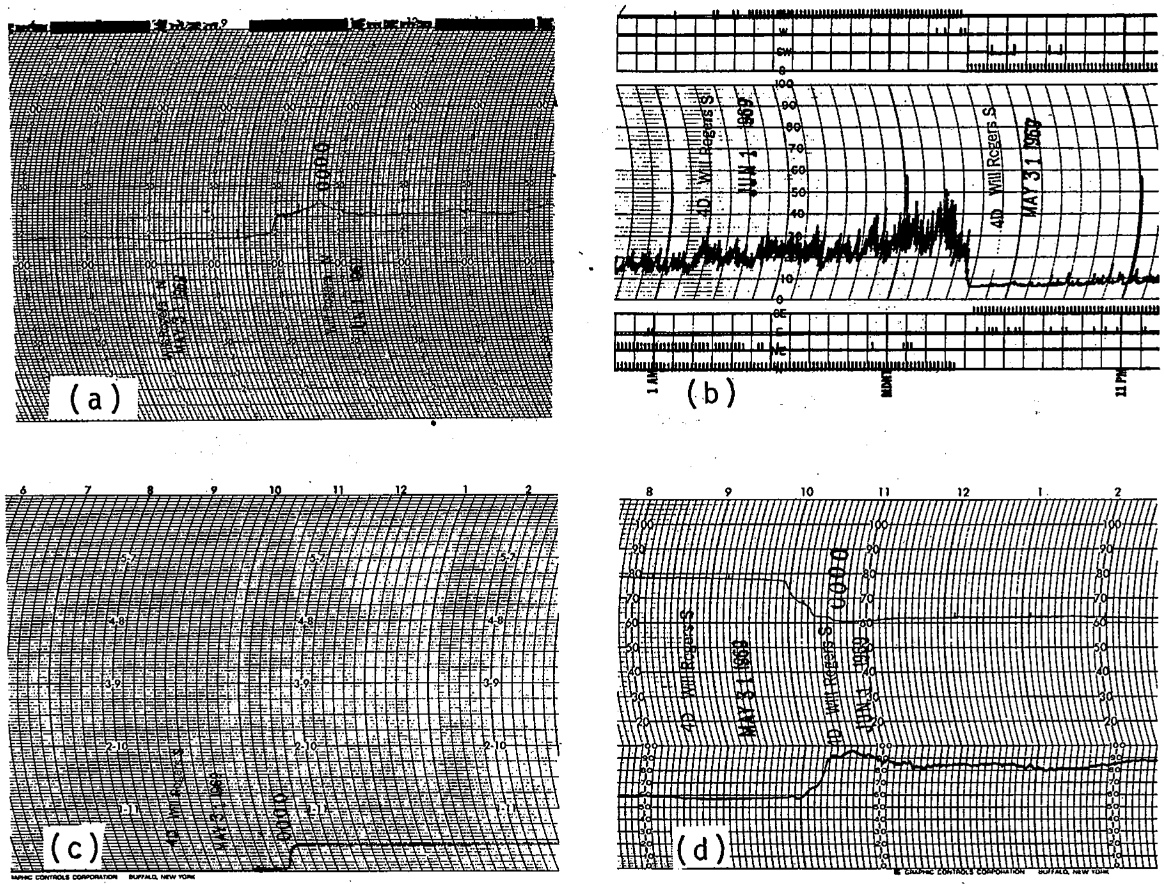

Figure 3. Examples of network data, (a) pressure, (b) wind, (c) precipitation, and (d) temperature-humidity.

The network has been operated during the severe storm season from April 1 to June 1. All stations are visited twice weekly for maintenance and calibration. In addition to changing the charts and comparing the wind recorder clock with a chronometer, the technician makes comparative observations of pressure, temperature, and humidity, to detect instrument drift and obvious malfunctions. These comparative data are catalogued by station and instrument, and corrections are applied to the data when they are analyzed. The differences in calibration times and chart markings are linearly interpolated by computer to adjust all records. An example of the correction printout included in preprocessed data sets is shown in table 2. The wind direction and speed sensors and the raingage are calibrated once before, once during, and once after the operational period.

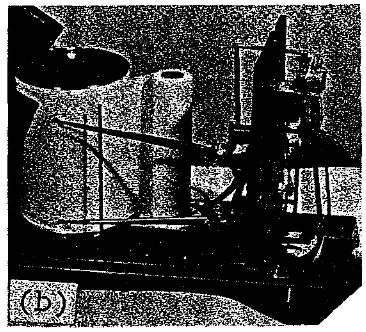

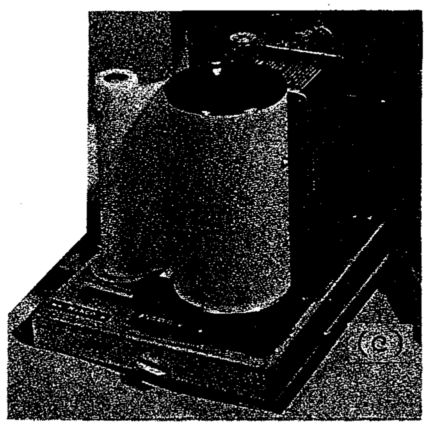

Figure 4. Modified (a) raingage, (b) hygrothermograph, (c) microbarograph.

3. OBSERVATIONS OF WIND GUSTS DURING SEVERE STORMS

The traces recorded during severe storm events are characteristically noisy, but conservative properties of the pressure, temperature, and wind velocity patterns become apparent after suitable averaging. This is well illustrated by a typical surface gust profile observed with a severe squall line. As shown in the cup anemometer record (fig. 3), the disturbance is often marked by a rapid build-up of wind speed, followed by its relatively slow decay in the post-storm environment. The period of interest (i.e., the period of potentially damaging wind) is about 30 min. Of course, the period depends on the horizontal depth of the gust front and the translational velocity of the squall line. The maximum wind gust experienced at a station is strongly influenced by local terrain. However, the variance of the speed is linearly related to the mean wind speed (Barclay and

Table 2. Example of Correction Printout of Processed Data.

STATION	DATE	TIME PRE-PRINTED ON WIND CHART	ABS. TIME OF PRE-PRINTED HR. LINE ON WIND CHART	ABS. TIME OF PENNED HR. MARK ON ALL CHARTS
5A	52770	000	8	7
5A	52770	100	108	107
5A	52770	200	208	207
5A	52770	300	308	307
5A	52770	400	409	408
5A	52770	500	509	508
5A	52770	600	609	608
5A	52770	700	709	708
5A	52770	800	810	809
5A	52770	900	910	909
5A	52770	1000	1010	1009
5A	52770	1100	1110	1109
5A	52770	1200	1210	1209
5A	52770	1300	1311	1310
5A	52770	1400	1411	1410
5A	52770	1500	1511	1510
5A	52770	1600	1611	1610
5A	52770	1700	1711	1710
5A	52770	1800	1812	1811
5A	52770	1900	1912	1911
5A	52770	2000	2012	2011
5A	52770	2100	2112	2111
5A	52770	2200	2212	2211
5A	52770	2300	2313	2312

Wilk, 1970), and the gusts can be estimated from the spatial analysis of the mean wind profile. The average direction and speed within the gust front are also related. The average wind direction veers steadily as the average speed increases.

That severe gusts are statistically rare is shown by the number of gusts that exceed selected thresholds. A search of continuous records for April, May, and June 1967 from a 58-station network covering 4000 sq miles disclosed that gusts greater than 50 kt occurred only 52 times on 13 days. Gusts greater than 35 kt occurred on 46 of the 90 days considered, with 14 of these on days having no thunderstorms. Of the gusts associated with thunderstorms, nine were with squall lines, 11 with cold fronts, nine with overrunning, and three with air mass thunderstorms.

The frequency distribution of the gusts (fig. 5) shows that gusts greater than 45 kt occur one-tenth as often as gusts of 35 kt, and that gusts greater than 55 kt occur only about 1 percent of the time when the gusts exceed 35 kt.

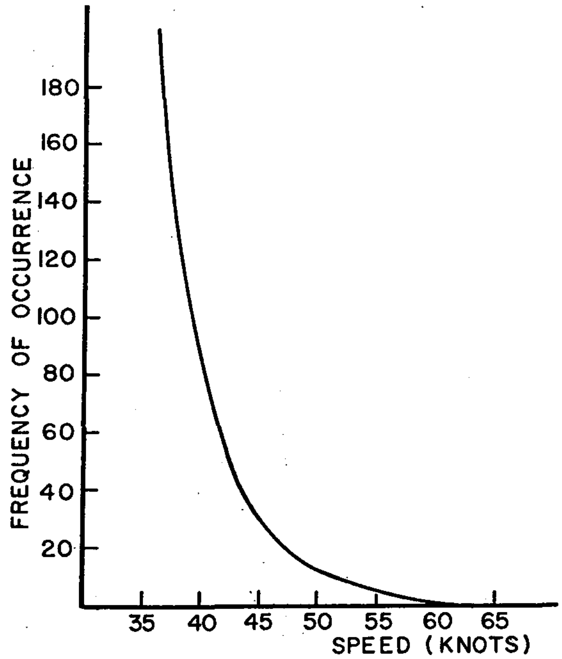

Figure 5. Frequency distribution of gusts > 35 kt.

Of course, widespread severe gusts occur most often with large scale severe thunderstorm outbreaks. Because of their great horizontal extent and relatively long lifetime, squall lines produce severe gusts over larger areas. The most intense gusts are associated with discrete cells, isolated or embedded in lines. With the isolated cells, the radar PPI display sometimes shows evidence of celular rotation which may culminate in a tornado cyclone. The following section illustrates both types of systems as they were portrayed by the NSSL surface network and WSR-57 weather radar.

4. SPATIAL ANALYSIS OF GUST FRONTS

Although the quantitative radar display is an alert for the possibility of severe weather, the forecasting of hazardous wind gusts is a four-fold problem of detection, interpretation, pattern extrapolation of the smoothed field, and the prediction of maximum gusts. The recognition and description of the gust profile are accomplished by sensing the sudden shift in direction and calculating average maximum speed (upper boundary of the wind envelope as shown on strip charts) during successive 5-min intervals for the 15 to 30 min period of strong gusts. The objective analysis of these data throughout the network for any specified 5-min period is readily completed by a grid interpolation and smoothing technique, such as proposed by Barnes (1964) or Sasaki (1970). The Barnes's technique, a convergent, weighted-averaging scheme was used by Barclay and Wilk (1970) to analyze the fields of maximum wind velocity.

Examples of the isotach and isogon fields that they obtained for the storm shown in figure 6(a) are reproduced in figures 6(b) and 6(c). These fields were constructed from 1-min values of maximum wind velocity which were linearly averaged for 5 min and space-interpolated using Barnes's technique. The smoothed field retains about 90 percent of the peak gust (5-min average) amplitudes.

A time sequence of the computer-listed isotach fields, objectively analyzed at 5-min intervals (fig. 7), clearly shows the movement of a speed-shear zone across the NSSL surface

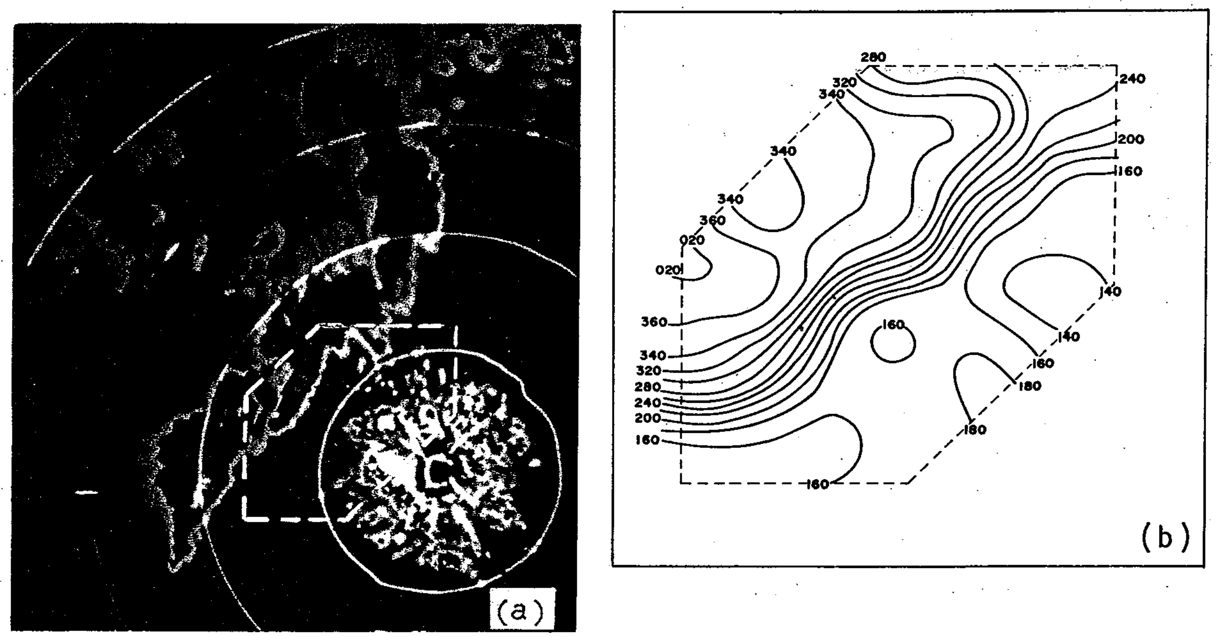

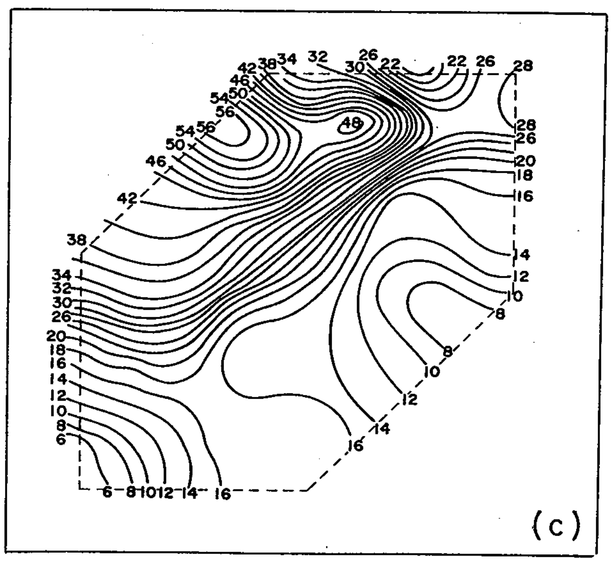

Figure 6. Examples of (a) radar display, (b) isogon analysis, and (c) isotach analysis for 2332 CST May 31, 1969.

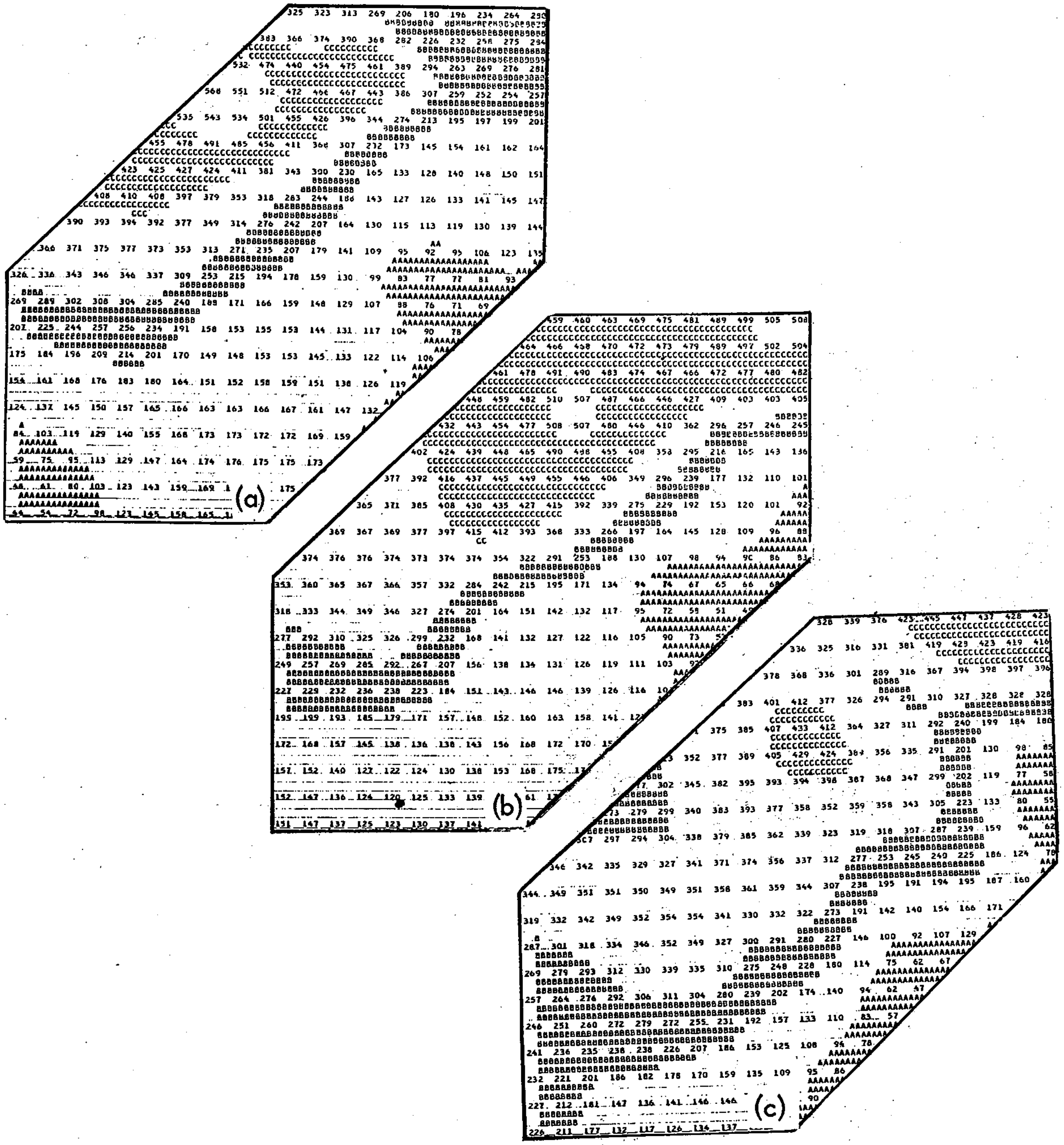

Figure 7. Time sequence of isotach fields for May 31, 1969. (a) 2337 CST, (b) 2342 CST, (c) 2347 CST.

network on May 31, 1969. To test the stability of this isotach pattern, we grouped the analyzed grid values in 5-kt class intervals and cross-correlated them at various spatial lags. The maximum correlation coefficient is a measure of the number of grid values matched at the best fit spatial lag. The contingency table derived from the matched pairs provides a measure of the agreement in each class of wind speed and indicates the areas in the isotach field that are stable with time. The correlation coefficient, as shown in figure 8(a), ranges from 0.4 for the 51 to 55 kt area to 0.85 for the 21 to 25 kt area. Figure 8(b), which shows the contingency results, shows that the observed data field persists over the 5-min period for speeds up to 40 kt with 80 percent of the values persisting. The percent of hits (i.e., number of matched pairs at the overall optimum spatial lag) decreases to less than 65 percent above 45 kt. By projecting for an additional 5 min, the spatial lag that gives the highest correlation coefficient one can determine the 5-min predictibility of the isotach field. The dashed line in figure 8(b) shows this predictability to be 5 to 10 percent lower than the optimum fit.

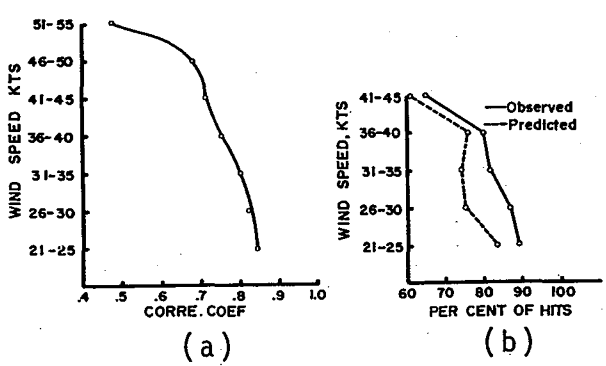

Figure 8. Stability analysis of isotach fields (a) correlation coefficient, (b) contingency results.

In this particular case, the shear zone moved from the northwest at 34 kt, while the isotach maximum moved from the southwest at approximately 50 kt. This differential motion caused the small area of strongest winds to be poorly matched when lagged by the velocity of the larger area of moderate winds. Irregularities in the motion of small, intense gust areas are expected, since the motions of the heavy rain cells often show differing tracks. The isotach maximum on May 31, 1969, moved more nearly with the velocity of the tall, intense thunderstorm.

5. SURFACE WIND ANALYSIS ON APRIL 29-30, 1970: THE OKLAHOMA CITY TORNADOES

The increased size of the 1970 network provided improved coverage for detection and analysis of severe gust events. The 44-station network and the 3.175 km^2 grid used for objective interpolation of the data are shown in figure 9.

As in 1969, the 1970 data were read from the strip chart records at 1-min intervals. In 1969, these values were read manually, whereas in 1970, the maximum and minimum values in each 1-min interval were read with a Benson-Lehner trace reader. The mean wind velocity was taken as the arithmetic average of the two limits, and the 5-min running average was calculated for use in the spatial analysis.

The storm of greatest interest in 1970, and probably the best documented tornadic storm in many years, occurred on April 29-30. Shortly after midnight an isolated severe

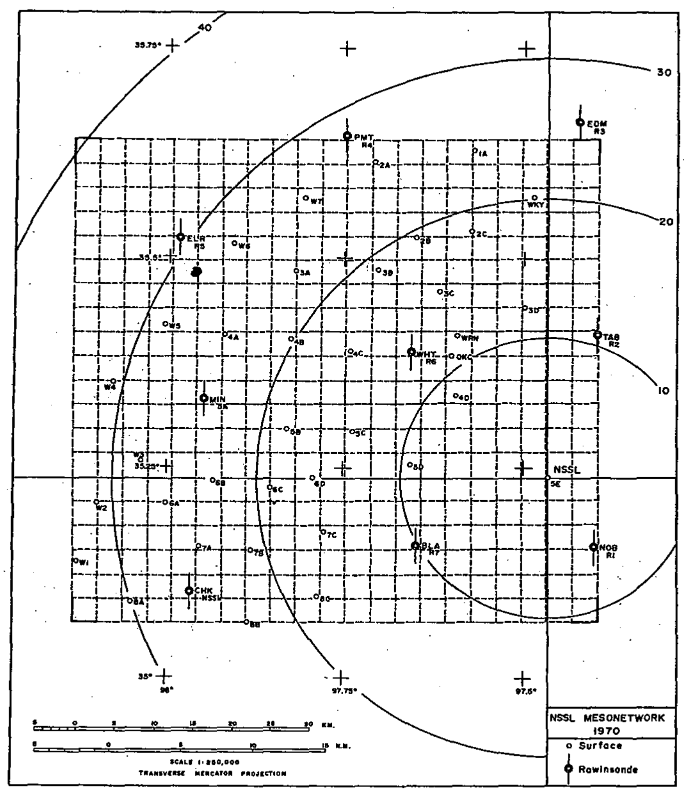

Figure 9. The NSSL 1970 meso-network with analysis grid.

thunderstorm produced a tornado that traveled across northern Oklahoma City. About 40 min later, another tornado accompanied a line of thunderstorms across the central part of the city. In both cases, the funnels passed between surface stations without damaging the equipment. The second funnel passed within a few hundred yards of station 4C, which registered a peak gust of 96 kt.

The isolated thunderstorm, figure 10(a), presented a characteristic hook in its WSR-57 radar display at 0043 CST as the storm passed across the northwestern edge of Oklahoma City. The corresponding surface wind velocity analysis (fig. 10(b)) maps the strong confluence associated with the boundary layer streamlines and delineates the 40 to 50 kt isotach maximum probably associated with the storm's outflow[1]. A few minutes after 0100 CST, this storm moved northeastward out of the network.

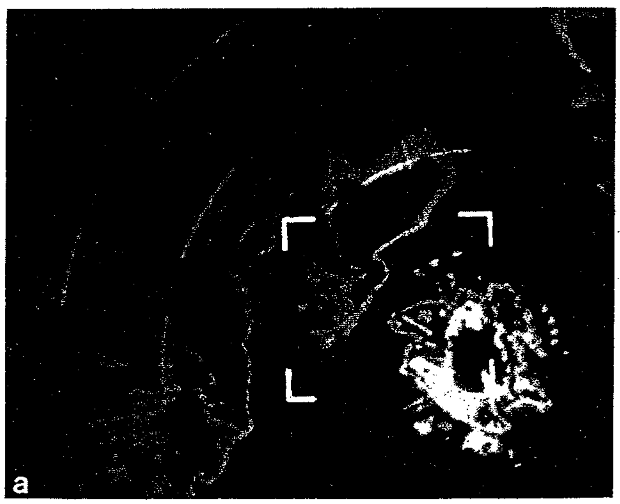

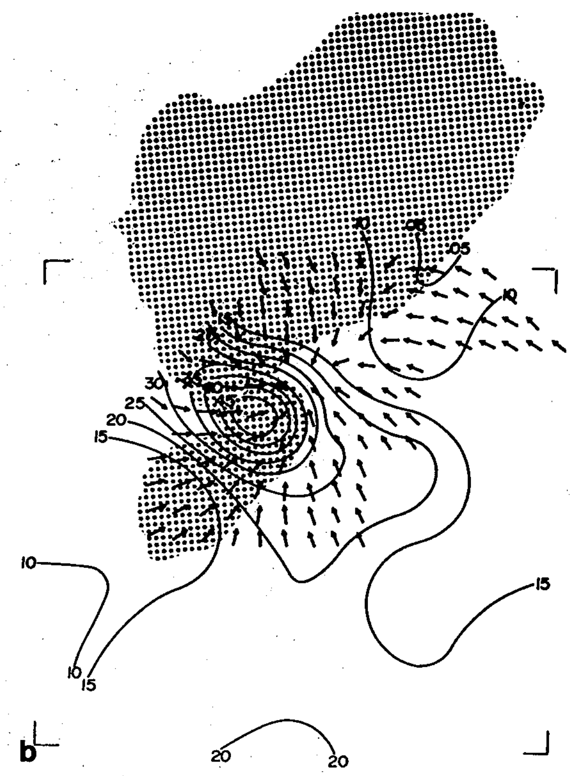

Figure 10. An example of (a) radar display, (b) corresponding surface wind analysis for 0043 CST April 30, 1970.

[1]The three-dimensional airflow can be determined only from a comprehensive analysis of all the surface, upper air, and radar observations currently being processed.

A line of thunderstorms followed the isolated storm over the network at 0104 CST, with the second tornado first occurring 16 min later near station 4C. In figure 11, the arrow marks the region of the second tornado cyclone. The first torando cyclone is still visible at 360 degrees at about 38 n miles.

The isotach maximum associated with the second tornado was first detected at the western edge of the network coincidentally with the arrival of the line. The subsequent 5-min streamline and isotach analyses are shown in figures 12(a) through (f). The confluence area remains northeast of the maximum wind gusts during the 25-min period.

When combined with the quantitative radar data, the sensibility of the surface wind field is remarkable. The pattern not only reflects the scale and circulation of the mesosystem

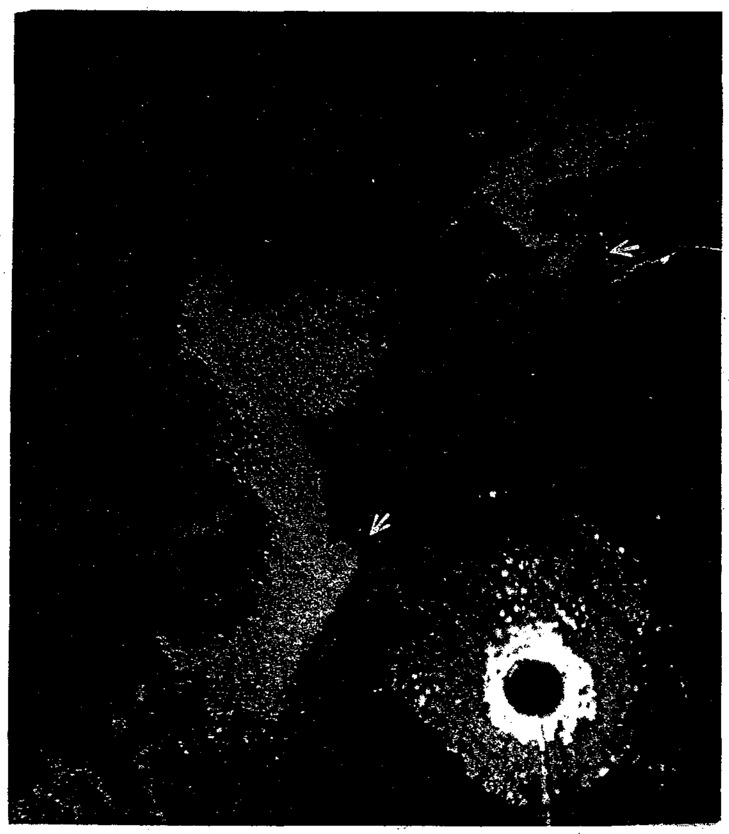

Figure 11. Radar display 0120 CST April 30, 1970.

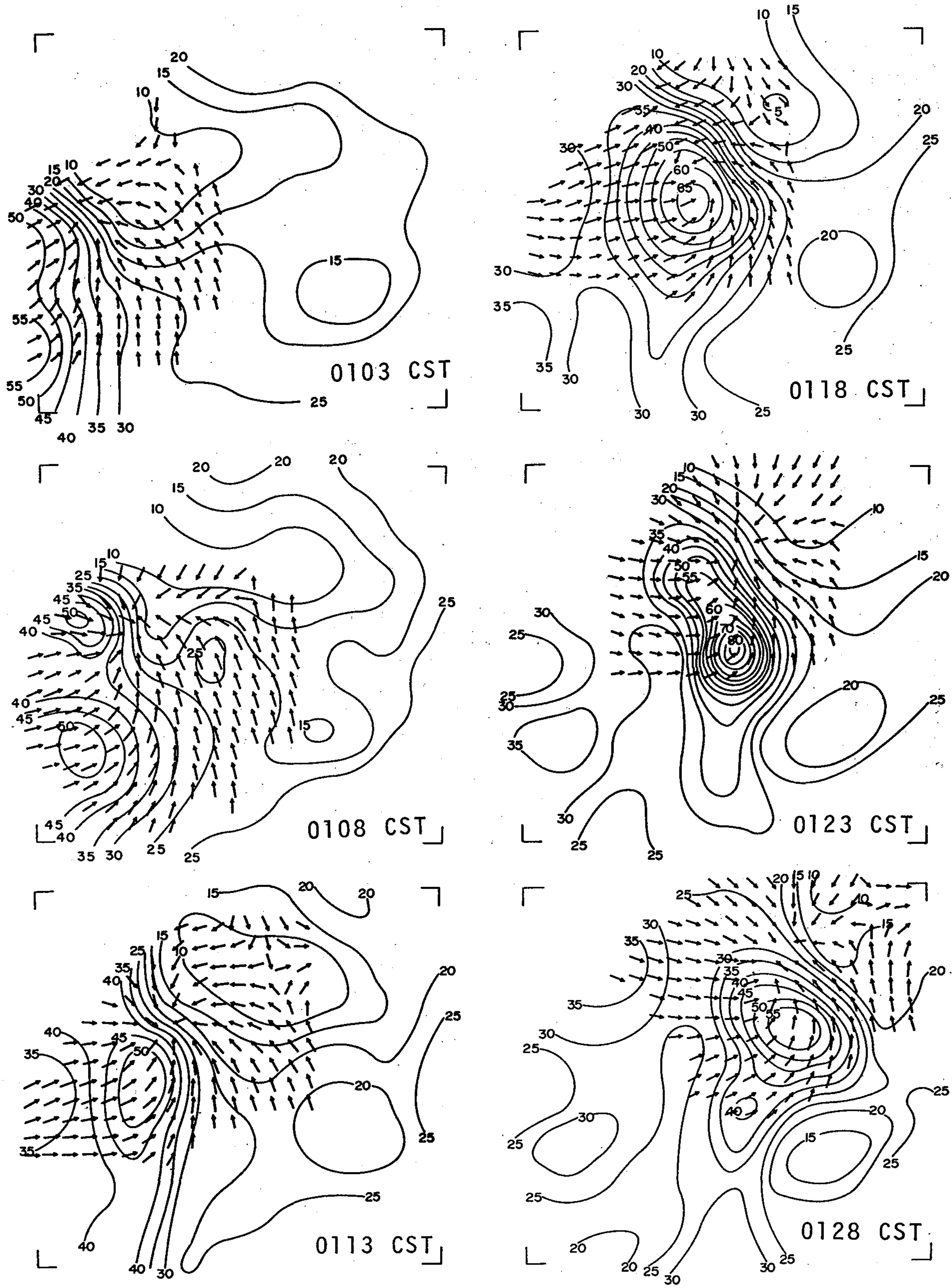

Figure 12. Time sequence of isotach and streamline analysis for April 30, 1970.

suggested by the radar echo, but also shows a translational stability similar to the precipitation area. Study of the surface wind data indicates that an operational network, with real time readout, would have reliably detected these severe wind events. The stability of the patterns produced by objective analysis shows that extrapolation of the pattern for 15 to 30 min is practical.

6. AN OPERATIONAL SYSTEM FOR REAL TIME DATA ACQUISITION

In all of the 1969-70 analyses, 1-min observations of the wind velocity acquired during gusty periods sufficiently defined the spatial wind field to warn of hazardous gusts. Also, the WSR-57 contoured radar data provided adequate information for identifying and tracking the associated severe thunderstorms (Wilk and Gray, 1970).

Our next goal in this project is to develop a remote data acquisition system capable of real time sampling, storing, and transmitting of meteorological information suitable for short-range forecasting. The configuration of the NSSL remote data acquisition system currently in use is shown in figure 13. For post analysis, the system records wind, temperature, humidity, pressure, and rainfall information in analog form on strip charts and stores digital samples on magnetic tape on site. As an alternate technique, we are considering a system with an acoustical coupler for monitoring the wind in real time, and transmitting data digitally to a central station. Normally, any given station will be activated only when the WSR-57 radar indicates severe thunderstorms are near the station.

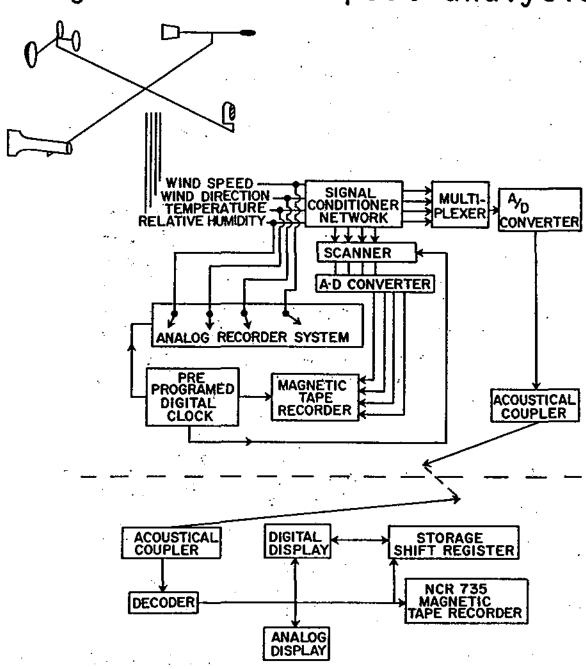

Figure 13. NSSL remote data acquisition system.

For operational tests of a "call-up" concept to obtain special wind observations during periods of severe weather, cooperative agreements should be established with general aviation airport operators to use wind sensors with standard indicators (and recorders, if desirable) that can be acoustically coupled for transmission of data to the National Severe Storms Laboratory. As shown in figure 14, the airports in Oklahoma offer a great potential as observational sites.

Using real time computer processing, available with comercial time share service, the National Weather Service hourly wind data and the special wind data can be combined in attempts to delineate mesoscale circulations under operational conditions. As stated previously, the contoured WSR-57 display would be used to determine the region of interest and the specific stations to be interrogated.

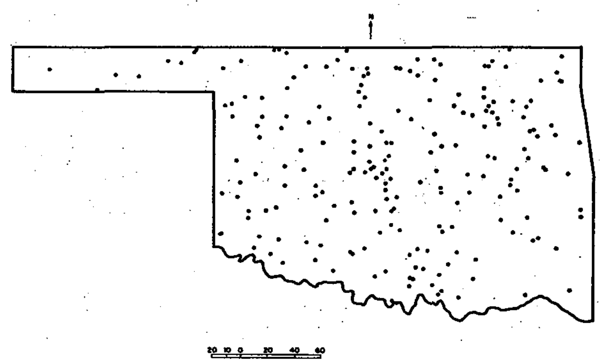

Figure 14. Map of airports in Oklahoma.

Research to improve operational observing and analyzing techniques can increase the efficiency of the present system while demonstrating the utility of new techniques and instruments for indirect probing of severe thunderstorms.

7. REFERENCES

Barclay, P. A., and K. E. Wilk (1970), Severe thunderstorm radar echo motion and related weather events hazardous to aviation operations, Tech. Memo. ERLTM-NSSL 46, 63 pp.

Barnes, S. L. (1964), A technique for maximizing details in numerical weather map analysis, J. Appl. Meteorol., 3, pp. 396-409.

Bonner, W. D. (1966), Case study of thunderstorm activity in relation to the low-level jet, Monthly Weather Review, 94, No. 3, pp. 167-178.

Brown, H. A. (1962), On the role of the humidity dip in squall line meso-systems, Unpublished Mss; paper presented at Amer. Meteorol. Soc. Conf. on Severe Storms, Norman, Okla.

Byers, H. R., and R. R. Braham, Jr. (1949), The Thunderstorm, (U. S. Gov't Printing Office, Washington, D. C.) 287 pp.

Charba, J., and Y. Sasaki, (1968), Structure and movement of the severe thunderstorms of 3 April 1964 as revealed from radar and surface mesonetwork data analysis, Tech. Memo ERLTM-NSSL 41, 47 pp.

Fujita, T. (1963), Analytical mesometeorology: a review, Meteorol. Monographs, 5, No. 27, Severe Local Storms, pp. 77-125.

Lemon, L. R. (1970), Formation and emergence of an anti-cyclonic eddy within a severe thunderstorm as revealed by radar surface data, Proceedings, 14th Weather Radar Conf., Tucson, Ariz. pp. 323-328.

Sasaki, Y. (1970), Numerical variational analysis with weak constraint and application to surface analysis of severe storm gust, Monthly Weather Review, 98, No. 12, pp. 899-910.

Styber, K. A., and R. H. Brown (1962), On the mesometeorological field studies near Flagstaff, Arizona, J. Appl. Meteorol., 1, pp. 26-42.

Wilk, K. E., and K. Gray (1970), Processing and analysis techniques used with the NSSL weather radar system, Proceedings, 14th Weather Radar Conf., Tucson, Ariz. pp. 369-374.

Williams, D. T. (1963), Analysis methods for small-scale surface network data, NSSP Report No. 17, U. S. Weather Bureau. 20 pp.

NATIONAL SEVERE STORMS LABORATORY

The NSSL Technical Memoranda, beginning with No. 28, continue the sequence established by the U. S. Weather Bureau National Severe Storms Project, Kansas City, Missouri. Numbers 1-22 were designated NSSP Reports. Numbers 23-27 were NSSL Reports, and 24-27 appeared as subseries of Weather Bureau Technical Notes. These reports are available from the National Technical Information Service, Operations Division, Springfield, Virginia 22151, for $3.00, and a microfiche version for $0.95. NTIS numbers are given below in parentheses.

No. 1 National Severe Storms Project Objectives and Basic Design. Staff, NSSP. March 1961. (PB-168207)

No. 2 The Development of Aircraft Investigations of Squall Lines from 1956-1960. B. B. Goddard. (PB-168208)

No. 3 Instability Lines and Their Environments as Shown by Aircraft Soundings and Quasi-Horizontal Traverses. D. T. Williams. February 1962. (PB-168209)

No. 4 On the Mechanics of the Tornado. J. R. Fulks. February 1962. (PB-168210)

No. 5 A Summary of Field Operations and Data Collection by the National Severe Storms Project in Spring 1961. J. T. Lee. March 1962. (PB-165095)

No. 6 Index to the NSSP Surface Network. T. Fujita. April 1962. (PB-168212)

No. 7 The Vertical Structure of Three Dry Lines as Revealed by Aircraft Traverses. E. L. McGuire. April 1962. (PB-168213)

No. 8 Radar Observations of a Tornado Thunderstorm in Vertical Section. Ralph J. Donaldson, Jr. April 1962. (PB-174859)

No. 9 Dynamics of Severe Convective Storms. Chester W. Newton. July 1962. (PB-163319)

No. 10 Some Measured Characteristics of Severe Storms Turbulence. Roy Steiner and Richard H. Rhyne. July 1962. (N62-16401)

No. 11 A Study of the Kinematic Properties of Certain Small-Scale Systems. D. T. Williams. October 1962. (PB-168216)

No. 12 Analysis of the Severe Weather Factor in Automatic Control of Air Route Traffic. W. Boynton Beckwith. December 1962. (PB-168217)

No. 13 500-Kc./Sec. Sferics Studies in Severe Storms. Douglas A. Kohl and John E. Miller. April 1963. (PB-168218)

No. 14 Field Operations of the National Severe Storms Project in Spring 1962. L. D. Sanders. May 1963. (PB-168219)

No. 15 Penetrations of Thunderstorms by an Aircraft Flying at Supersonic Speeds. G. P. Roys. Radar Photographs and Gust Loads in Three Storms of 1961 Rough Rider. Paul W. J. Schumacher. May 1963. (PB-168220)

No. 16 Analysis of Selected Aircraft Data from NSSP Operations, 1962. T. Fujita. May 1963. (PB-168221)

No. 17 Analysis of Methods for Small-Scale Surface Network Data. D. T. Williams. August 1963. (PB-168222)

No. 18 The Thunderstorm Wake of May 4, 1961. D. T. Williams. August 1963. (PB-168223)

No. 19 Measurements by Aircraft of Condensed Water in Great Plains Thunderstorms. George P. Roys and Edwin Kessler. July 1966. (PB-173048)

No. 20 Field Operations of the National Severe Storms Project in Spring 1963. J. T. Lee, L. D. Sanders and D. T. Williams. January 1964. (PB-168224)

No. 21 On the Motion and Predictability of Convective Systems as Related to the Upper Winds in a Case of Small Turning of Wind with Height. James C. Fankhauser. January 1964. (PB168225)

No. 22 Movement and Development Patterns of Convective Storms and Forecasting the Probability of Storm Passage at a Given Location. Chester W. Newton and James C. Fankhauser. January 1964. (PB-168226)

No. 23 Purposes and Programs of the National Severe Storms Laboratory, Norman, Oklahoma. Edwin Kessler. December 1964. (PB-166675)

No. 24 Papers on Weather Radar, Atmospheric Turbulence, Sferics, and Data Processing. August 1965. (AD-621586)

No. 25 A Comparison of Kinematically Computed Precipitation with Observed Convective Rainfall. James C. Fankhauser. September 1965. (PB-168445).

No. 26 Probing Air Motion by Doppler Analysis of Radar Clear Air Returns. Roger M. Lhermitte. May 1966. (PB-170636)

No. 27 Statistical Properties of Radar Echo Patterns and the Radar Echo Process. Larry Armijo. May 1966. The Role of the Kutta-Joukowski Force in Cloud Systems with Circulation. J. L. Goldman. May 1966. (PB-170756)

No. 28 Movement and Predictablity of Radar Echoes. James Warren Wilson. November 1966. (PB-173972)

No. 29 Notes on Thunderstorm Motions, Heights, and Circulations. T. W. Harrold, W. T. Roach, and Kenneth E. Wilk. November 1966. (AD-644899)

No. 30 Turbulence in Clear Air Near Thunderstorms. Anne Burns, Terence W. Harrold, Jack Burnham, and Clifford S. Spavins. December 1966. (PB-173992)

No. 31 Study of a Left-Moving Thunderstorm of 23 April 1964. George R. Hammond. April 1967. (PB-174681)

No. 32 Thunderstorm Circulations and Turbulence from Aircraft and Radar Data. James C. Fankhauser and J. T. Lee. April 1967. (PB-174860)

No. 33 On the Continuity of Water Substance. Edwin Kessler. April 1967. (PB-175840)

No. 34 Note on the Probing Balloon Motion by Doppler Radar. Roger M. Lhermitte. July 1967. (PB-175930)

No. 35 A Theory for the Determination of Wind and Precipitation Velocities with Doppler Radars. Larry Armijo. August 1967. (PB-176376)

No. 36 A Preliminary Evaluation of the F-100 Rough Rider Turbulence Measurement System. U. O. Lappe. October 1967. (PB-177037)

No. 37 Preliminary Quantitative Analysis of Airborne Weather Radar. Lester P. Merritt. December 1967. (PB-177188)

No. 38 On the Source of Thunderstorm Rotation. Stanley L. Barnes. March 1968. (PB-178990)

No. 39 Thunderstorm - Environment Interactions Revealed by Chaff Trajectories in the Mid-Troposphere. James C. Fankhauser. June 1968. (PB-179659)

No. 40 Objective Detection and Correction of Errors in Radiosonde Data. Rex L. Inman. June 1968. (PB-180284)

No. 41 Structure and Movement of the Severe Thunderstorms of 3 April 1964 as Revealed from Radar and Surface Mesonetwork Data Analysis. Jess Charba and Yoshikazu Sasaki. October 1968. (PB-183310)

No. 42 A Rainfall Rate Sensor. Brian E. Morgan. November 1968. (PB-183979)

No. 43 Detection and Presentation of Severe Thunderstorms by Airborne and Ground-Based Radars: A Comparative Study. Kenneth E. Wilk, John K. Carter, and J. T. Dooley. February 1969. (PB-183572)

No. 44 A Study of a Severe Local Storm of 16 April 1967. George Thomas Haglund. May 1969. (PB-184-970)

No.45 On the Relationship Between Horizontal Moisture Convergence and Convective Cloud Formation. Horace R. Hudson. March 1970. (PB-191720)

No. 46 Severe Thunderstorm Radar Echo Motion and Related Weather Events Hazardous to Aviation Operations. Peter A. Barclay and Kenneth E. Wilk. June 1970. (PB-192498)

No. 47 Evaluation of Roughness Lengths at the NSSL-WKY Meteorological Tower. Leslie D. Sanders and Allen H. Weber. August 1970. (PB-194587)

No. 48 Behavior of Winds in the Lowest 1500 ft in Central Oklahoma: June 1966 - May 1967. Kenneth C. Crawford and Horace R. Hudson. August 1970.

No. 49 Tornado Incidence Maps. Arnold Court. August 1970. (COM-71-00019)

No. 50 The Meteorologically Instrumented WKY-TV Tower Facility. John K. Carter. September 1970. (COM-71-00108)

No. 51 Papers on Operational Objective Analysis Schemes at the National Severe Storms Forecast Center. Rex L. Inman. November 1970. (COM-71-00136)

No.52 The Exploration of Certain Features of Tornado Dynamics Using a Laboratory Model. Neil B. Ward. November 1970. (COM-71-00139)

No.53 Rawinsonde Observation and Processing Techniques at the National Severe Storms Laboratory. Stanley L. Barnes, James H. Henderson and Robert J. Ketchum. April 1971.

No. 54 Model of Precipitation and Vertical Air Currents. Edwin Kessler and William C. Bumgarner. June 1971.

☆ U.S. GOVERNMENT PRINTING OFFICE: 1974 — 677-238 / 1238 REGION NO. 8